Available online at www.sciencedirect.com
SCIENCE DIRECT
Biochimica et Biophysica Acta 1712 (2005) 197 – 211
BIOCHIMICA ET BIOPHYSICA ACTA
BBA
http://www.elsevier.com/locate/bba

Bilayer interaction and localization of cell penetrating peptides with model membranes: A comparative study of a human calcitonin (hCT)-derived peptide with pVEC and pAntp(43–58)

Michael E. Herbig[a], Ursina Fromm[a], Jeannine Leuenberger[a], Ulrike Krauss[b], Annette G. Beck-Sickinger[b], Hans P. Merkle[a,*]

[a]*Drug Formulation and Delivery Group, Department of Chemistry and Applied BioSciences, Swiss Federal Institute of Technology Zurich (ETH Zurich), Wolfgang-Pauli-Strasse 10, CH-8093 Zurich, Switzerland*
[b]*Institute of Biochemistry, University of Leipzig, Bruderstrasse 34, D-04103 Leipzig, Germany*

Received 22 February 2005; received in revised form 7 April 2005; accepted 18 April 2005
Available online 6 May 2005

Abstract

Cell-penetrating peptides (CPPs) are able to translocate problematic therapeutic cargoes across cellular membranes. The exact mechanisms of translocation are still under investigation. However, evidence for endocytic uptake is increasing. We investigated the interactions of CPPs with phospholipid bilayers as first step of translocation. To this purpose, we employed four independent techniques, comprising (i) liposome buffer equilibrium dialysis, (ii) Trp fluorescence quenching, (iii) fluorescence polarization, and (iv) determination of ζ-potentials. Using unilamellar vesicles (LUVs) of different phospholipid composition, we compared weakly cationic human calcitonin (hCT)-derived peptides with the oligocationic CPPs pVEC and penetratin (pAntp). Apparent partition coefficients of hCT-derived peptides in neutral POPC LUVs were dependent on amino acid composition and secondary structure; partitioning in negatively charged POPC/POPG (80:20) LUVs was increased and mainly governed by electrostatic interactions. For hCT(9–32) and its derivatives, *D* values raised from about 100–200 in POPC to about 1000 to 1500 when negatively charged lipids were present. Localization profiles of CPPs obtained by Trp fluorescence quenching were dependent on the charge density of LUVs. In POPC/POPG, hCT-derived CPPs were located on the bilayer surface, whereas pVEC and pAntp resided deeper in the membrane. In POPG LUVs, an increase of fluorescence polarization was observed for pVEC and pAntp but not for hCT-derived peptides. Generally, we found strong peptide–phospholipid interactions, especially when negatively charged lipids were present.

Keywords: Cell penetrating peptides; Fluorescence spectroscopy; Liposome–buffer partitioning; Lipid bilayer models; Phospholipid vesicles; Peptide–lipid interactions

1. Introduction

Over the past decade, several classes and/or prototypes of cell-penetrating peptides (CPPs) have been characterized in several aspects. Initially, their entry mechanisms were postulated not to be mediated by receptors or transporters [1,2], suggesting a passive, non-endocytic transfer. More recently, however, increasing evidence has been brought up suggesting the involvement of active, endocytic processes [3–7]. The ability of the CPPs to translocate when covalently or physically linked with a cargo, including polypeptides and nucleic acids, renders them of broad interest in cell biology, biotechnology and drug delivery. In

Abbreviations: CPP, cell penetrating peptide; hCT, human calcitonin; pVEC, vascular endothelial cadherin-derived CPP; pAntp, penetratin, Antennapedia homeodomain-derived CPP; POPC, 1-palmitoyl-2-oleoyl-phosphatidylcholine; POPG, 1-palmitoyl-2-oleoyl-phosphatidylglycerol; DPC, dodecyl phosphocholine; Br-PC, 1-palmitoyl-2-stearoyl-(11,12-dibromo)-*sn*-glycero-3-phosphocholine; NBD-PE, N-(7-nitrobenzofurazan-4-yl)-1,2-dipalmitoyl-*sn*-glycero-3-phosphoethanolamine; 5-DSA, 5-doxylstearic acid; DPH, 1,6-diphenyl-1,3,5-hexatriene; TFA, trifluoroacetic acid; PBS, phosphate-buffered saline; RP-HPLC, reversed phase HPLC; LUV, large unilamellar vesicles; SUV, small unilamellar vesicles; MLV, multilamellar vesicles; DLS, dynamic light scattering; K_{SV}, Stern–Volmer constant

* Corresponding author. Tel.: +41 44 6337310; fax: +41 44 6337314.
E-mail address: hmerkle@pharma.ethz.ch (H.P. Merkle).

0005-2736/$ - see front matter © 2005 Elsevier B.V. All rights reserved.
doi:10.1016/j.bbamem.2005.04.006

fact, CPPs have been used as vectors for the cytoplasmic and nuclear delivery of hydrophilic biomolecules and drugs, both in vivo and in vitro [1,2,8]. The exact mechanisms underlying the translocation across membranes are still under investigation. As a consequence of artifactual uptake phenomena due to cell fixation, the hypothesis of an energy independent, direct transport of CPPs trough biomembranes, postulated in earlier CPP studies [9–11], had to give way to concepts involving endocytosis [3–6,12]. Increasing attention is concentrated on the first step of CPP uptake: an initial adherence on the membrane surface leading to an enrichment in the phospholipid bilayer, which may subsequently trigger endocytic uptake [3,5,12–15]. In fact, in the few studies combining cell biological and biophysical approaches, good correlations between membrane affinity and uptake efficiency could be observed [16,17]. This underlines that both the cell biology of the uptake and the biophysical analysis of the interactions between the CPPs and the bilayer membrane are legitimate approaches necessary for a better understanding of CPP translocation mechanisms.

In the present study, we investigate in detail the interactions of two classes of CPPs with several bilayer models with the aim to contribute to the mechanistic understanding of such interactions as a step towards cellular translocation. Four independent methodological approaches were employed, comprising liposome buffer equilibrium dialysis, Trp fluorescence quenching, fluorescence polarization, and determination of ζ-potentials. In particular, we compared weakly cationic C-terminal fragments of human calcitonin, hCT(9–32) and modifications thereof with two oligocationic CPPs, the vascular endothelial (VE)-cadherin-derived CPP, pVEC, and the Antennapedia homeodomain protein-derived penetratin, denoted pAntp (Table 1).

Human calcitonin (hCT) is a peptide hormone that is approved for the treatment of established osteoporosis [18]. N-terminally truncated derivatives of hCT, which lack hormonal activity, represent a novel class of weakly cationic CPPs and have been systematically investigated by Tréhin et al. It has been shown that sequences from hCT(9–32) to hCT(18–32) penetrated the plasma membrane of a fully organized epithelial model, differentiated MDCK monolayers, and resulted in a sectoral, vesicular cytoplasmic distribution. The uptake process was temperature-, time-, and concentration-dependent, indicating that translocation may follow an endocytic pathway; among the investigated derivatives, hCT(9–32) was the most efficient one, and its single, positively charged lysine in position 18 turned out to be essential for uptake [19]. Furthermore, uptake was found to be cell-line specific with a punctuated, cytoplasmic pattern in MDCK cells and paracellular accumulation in Calu-3 cell monolayers. Remarkably, hCT-derived peptides did not show significant permeation across the epithelial models [20]. This owes to their efficient metabolic cleavage when in contact with the epithelial cells [21].

Cadherins are single transmembrane-spanning glycoproteins of about 700 amino acids. pVEC, a peptide derived from the murine VE-cadherin, contains 18-amino acids (residues 615–632), with 13 cytosolic amino acids outside and 5 amino acids in the transmembrane region. It has been shown to translocate efficiently into various cell lines by a receptor-independent mechanism, and to carry macromolecular cargoes through plasma membranes [22,23]. The sequence of pAntp corresponds to the 16 amino acid sequence of the third α-helix (residues 43–58) of the Antennapedia homeodomain protein of *Drosophila* [24,25]. Residues 48 and 56 are tryptophans (Trp) being useful fluorescent probes for biophysical analysis. The third helix was found to be responsible for interaction with DNA by binding specifically to cognate sites in the genome and also for the translocation of the entire protein across cell membranes [24,25]. The fragment pAntp retains the membrane translocation properties of the homeodomain and has, therefore, been proposed as a universal vector for cellular delivery [2]. In fact, there are numerous studies proving the translocation of pAntp into different cell lines [26,27]. More recent studies propose an endocytic uptake [15,16]. Its exact translocation mechanism is still controversially discussed as reviewed by Trehin and Merkle [3].

To our knowledge, the present study provides the first investigation of a direct interaction of hCT-derived peptides and pVEC with bilayer models. Indirectly, interactions of hCT-derived CPPs have been suggested by atomic force

Table 1
Abbreviations, amino acid sequences and molecular weight of the peptides studied in this work

Abbreviation	MW (Da)	Sequence
hCT	3417.8	CGNLS TCMLG TYTQD FNKFH TFPQT AIGVG AP-NH_2
hCT(9–32)	2609.9	LG TYTQD FNKFH TFPQT AIGVG AP-NH_2
W10-hCT(9–32)	2739.0	L<u>W</u> TYTQD FNKFH TFPQT AIGVG AP-NH_2
A23-hCT(9–32)	2583.8	LG TYTQD FNKFH TF<u>A</u>QT AIGVG AP-NH_2
W30-hCT(9–32)	2739.0	LG TYTQD FNKFH TFPQT AIGV<u>W</u> AP-NH_2
hCT(18–32)	1698.9	KFH TFPQT AIGVG AP-NH_2
hCT(21–32)	1286.4	TFPQT AIGVG AP-NH_2
hCT-random	2609.9	FL TAGQN TIQTP VKTGG HFPFA DY-NH_2
pVEC	2208.7	LLIIL RRRIR KQAHA HSK-NH_2
W2-pVEC	2281.7	L<u>W</u>IIL RRRIR KQAHA HSK-NH_2
pAntp	2246.7	RQIKI WFQNR RMKWK K

Amino acid substitutions are underlined.

microscopy on phase separated supported bilayers [28]. The interaction of pAntp with model membranes, on the other hand, has been investigated in numerous studies [10,17,29–31]. Its inclusion in this study was in order to allow comparison with previous data. In addition to that, we also provide new data to this peptide. Furthermore, we like to draw attention to methods that are suited to detect comparably weak associations of peptides with the outer surface of the bilayer. So far, biophysical analysis of CPP was largely focused on insertions into the hydrophobic core of the bilayer, and mere association with the surface of membranes was mostly neglected. Nevertheless, even weak forms of association may be the first step to trigger cellular uptake. Another focus of this work is a comprehensive Trp fluorescence quenching study on the localization and insertion of the investigated CPPs in phospholipid bilayers of various compositions. A total of four quenchers were looked at in order to monitor (i) interaction with the water phase, (ii) with the surface of the bilayer, (iii) the interface, and (iv) the hydrophobic core of the bilayer. Although all investigated CPPs showed marked affinities towards phospholipid bilayers, especially for negatively charged lipids, distinct differences in the type and extent of interaction between weakly cationic hCT-derived and oligocationic CPPs could be revealed.

2. Materials and methods

2.1. Materials

The VE-cadherin-derived peptides were synthesized by NMI Peptides, Reutlingen, Germany; hCT was kindly provided by Novartis Pharma AG, Basle, Switzerland. All peptides were amidated in the N-terminus. Identity and purity (>95%) were controlled by mass spectral and HPLC analysis. 1-palmitoyl-2-oleoyl-phosphatidylcholine (POPC), 1-palmitoyl-2-oleoyl-phosphatidylglycerol (POPG), dodecyl phosphocholine (DPC), and 1-palmitoyl-2-stearoyl-(11,12-dibromo)-*sn*-glycero-3-phosphocholine (Br-PC) were purchased from Avanti Polar Lipids (Alabaster, Alabama, USA), of the best quality available, and used without further purification. Trifluoroacetic acid (TFA), acrylamide, and 5-doxyl stearic acid (5-DSA) were from Fluka, Buchs, Switzerland. N-(7-nitrobenzofurazan-4-yl)-1,2-dipalmitoyl-*sn*-glycero-3-phosphoethanolamine (NBD-PE). 1,6-diphenyl-1,3,5-hexatriene (DPH) was purchased from Molecular Probes, Leiden, the Netherlands. Acetic acid (reagent grade) and phosphate-buffered saline (PBS) for buffer preparation were purchased from Fluka, Buchs, Switzerland.

2.2. Synthesis and purification of hCT-derived peptides

The sequences of the investigated hCT-derived peptides are given in Table 1. The peptides were synthesized by automated multiple solid phase peptide synthesis using a robot system (Syro, MultiSynTech, Bochum, Germany) and Fmoc/tert. butyl strategy as described previously [32]. Peptides were then purified by preparative reversed phase high performance liquid chromatography (RP-HPLC, Merck KGaA, Darmstadt, Germany) and their purity was confirmed by analytical RP-HPLC using a LiChrospher 100 RP-18 column (125 mm × 4 mm, 5 μM) from Merck (Merck KGaA, Darmstadt, Germany) with a linear gradient mobile phase starting at 90% solvent A (water/TFA, 99.9:0.1) (v/v) and 10% solvent B (acetonitrile/TFA, 99.92:0.08) (v/v) to 60% solvent B over 30 min at a flow rate of 1 mL/min. UV detection was monitored at 220 nm. The expected molecular weight was verified by MALDI-mass spectrometry (Voyager Perseptive, Weiterstadt, Germany). The analytical data for the not yet described derivatives were as follows: W10-hCT(9–32): $mass_{calc.}$ 2739.0 Da, $mass_{exp.}$ 2740.83 Da, HPLC retention time 19.95 min; A23-hCT(9–32): $mass_{calc.}$ 2583.8 Da, $mass_{exp.}$ 2584.90 Da, 19.41 min; W30-hCT(9–32): $mass_{calc.}$ 2739.0 Da, $mass_{exp.}$ 2740.72 Da, 20.75 min.

2.3. Preparation of unilamellar vesicles and micelles

Large unilamellar vesicles (LUVs) were prepared by dissolving the phospholipids, either pure, or in the desired molar ratio, in chloroform to ensure complete solution and mixing of the components. The lipids were dried at 37 °C in a rotary evaporator to yield a thin film and then kept under high vacuum over night. The dry film was then redispersed in the respective buffer (PBS, pH 7.4, 10 mM phosphate or acetic acid buffer, pH 3.5, 100 mM acetate) and the resulting multilamellar vesicle (MLV) dispersion was treated by five freeze–thaw cycles in liquid nitrogen and water at 37 °C. LUVs were obtained by extruding the MLVs four times through 0.4 μm and eight times through 0.1 μm Nuclepore polycarbonate membranes (Sterico, Wangen, Switzerland) by means of the Lipex extruder (Vancouver, Canada). Lipid concentration was determined by an enzymatic colorimetric test for phospholipids (MPR 2) obtained from Roche Diagnostics, Mannheim, Germany. To assure the quality of the liposomes, the LUV size was checked by photon correlation spectroscopy on a Zetasizer 3000 HSA (Malvern, Malvern, UK).

To obtain small unilamellar vesicles (SUVs), MLVs were prepared as described for LUVs. After five freeze–thaw cycles, in addition, the ice-cooled dispersion was sonicated under nitrogen, using a Digitana UP 200 H tip sonicator (Digitana, Horgen, Switzerland). The sonication was performed in 15 cycles of 1 min each at 60% amplitude and 100% duty cycle, followed by a 1-min pause to allow the dispersion to cool down. Titanium debris and lipid particles were removed by centrifugation at 10 000 × *g* during 25 min using a Beckman L-60 ultracentrifuge (Beckman-Coulter, Palo Alto, USA). The size of the resulting SUVs obtained by DLS analysis was 33.5 ± 1.32 nm (volume distribution).

Micelles of approximately 4 nm in diameter were obtained by dissolving DPC in PBS buffer.

2.4. Liposome–buffer partitioning experiments

Liposome–buffer partitioning experiments were performed by equilibrium dialysis at 37 °C during 7 h; 1 mL Teflon dialysis cells (Dianorm, Munich, Germany) separated by a cellulose dialysis membrane, molecular weight-cutoff 10,000 by Dianorm were mounted within the Dianorm-4 drive cell carrier and gently shaken during dialysis. Chambers were filled with a liposome suspension at a total lipid concentration of 4 mM in a 10-mM acetic acid buffer, pH 3.5, containing peptides at a concentration of 20 μM on the one and acetate buffer on the other side [33]. An acidic pH was chosen, as hCT-derived peptides occasionally aggregated at pH 7.4 under the conditions used for partitioning studies. For VE-cadherin-derived peptides PBS buffer of pH 7.4 was used. Schmidt et al. [34] could previously show that equilibrium was reached after 7 h. Over this time range, good stability of the phosphatidylcholine liposomes at 37 °C has been reported by Ottiger and Wunderli-Allenspach [35]. For HPLC analysis, liposomes were dissolved in methanol (1:3, v/v). The HPLC method described by Buck and Maxl [36] was applied with some modifications. Mobile phases consisted of water/acetonitrile/TFA, 899:100:1 (v/v) for A and 199:800:1 (v/v) for B. A linear gradient from 100% A to 100% B within 35 min was applied. A RP-18 capillary column (LiChroCART® 250-4, LiChropher® 100, RP-18 (5 μm), Merck, Darmstadt, Germany) was used. UV detection was set at 214 nm; for Trp containing peptides, an additional fluorescence detector was employed (excitation 280 nm, emission 320 nm). Injection volume was 100 μL. Throughout values at 7 h were used for calculation of apparent partition coefficients (D) which were calculated according to:

$$D = \frac{C_{P(b)}}{C_{P(f)} \cdot C_L} \tag{1}$$

where $C_{P(b)}$ is the concentration of peptide bound to liposomes, $C_{P(f)}$ the concentration of free peptide, and C_L is the concentration of lipid molecules. $C_{P(b)}$ was calculated by subtracting the peptide concentration in the buffer compartment from the peptide concentration in the liposome compartment.

2.5. Zeta-potential measurements

The zeta potential (ζ) of the liposomes was determined by laser Doppler electrophoresis using a Malvern ZetaSizer 3000 HS (Malvern Instruments Ltd., Malvern, UK) equipped with a He-Ne ion laser (633 nm). From the obtained electrophoretic mobility, the zeta potential was calculated using the Smoluchowski equation as follows:

$$\zeta = \frac{4\pi\eta u}{\varepsilon} \tag{2}$$

where u is the electrophoretic mobility, η the viscosity of the solvent, and ε the dielectric constant of the solvent. The reported results are expressed as mean values (±S.D.) of three experiments. The instrument was calibrated with a −50 mV standard (DTS1050; Malvern Instruments Ltd.). Measurements were performed at 20 °C with an electrical field strength of 150 V/cm. Samples at a fixed lipid concentration of 50 μM and peptide/lipid ratios ranging from 1:1000 to 1:10 were incubated for 1 h at room temperature.

2.6. Dynamic light scattering (DLS)

The size distribution of a 50-μM LUV alone or after 60 min incubation at 22 °C at variable concentrations of peptide was determined by dynamic light scattering (DLS) at a scattering angle of 90° on a Malvern ZetaSizer 3000 HS (Malvern Instruments Ltd., Malvern, UK) equipped with a He-Ne ion laser (633 nm). Hydrodynamic diameters (d_H, nm) were calculated from the diffusion coefficient (D) using the Stokes–Einstein equation:

$$d_H = \frac{kT}{3\pi\eta D} \tag{3}$$

where k is the Boltzmann constant; T the absolute temperature (K) and η the viscosity (mPa·s $^{-1}$) of the solvent. The correlation function was analysed by the CONTIN method and the intensity distribution was chosen for evaluation of the data.

2.7. Fluorescence spectroscopy

Fluorescence was measured on a Varian Cary Eclipse spectrofluorometer (Mulgrave, Australia). All measurements were made in 10 mm wide 40 μL micro-cuvettes at an ambient temperature of approximately 20 °C. To guarantee exclusive Trp excitation when measuring Trp fluorescence, the excitation wavelength was set to 295 nm and the emission scanned from 300 to 500 nm. For quenching experiments, the excitation wavelength was set to 375 nm. Scans were recorded with 5 nm excitation and emission bandwidths and a scan speed of 600 nm min $^{-1}$. Three scans were recorded and averaged for each sample. For DPH analyses, fluorescence was excited at 340 nm and the emission was determined at 452 nm; five measurements were performed and averaged for each sample.

2.7.1. Acrylamide and spin-probe quenching

Trp fluorescence quenching experiments were performed at a fixed lipid/peptide ratio (L/P) of 100 with peptide concentrations of 10 μM in presence of LUVs at a total phospholipid concentration of 1 mM. Acrylamide, a quenching molecule for Trp residues exposed to the water phase, was added from an aqueous 1 M stock solution, resulting in concentrations between 10 and 100 mM. For all samples containing vesicles, background intensity was

subtracted. Quenching efficiency (F_0/F) was calculated by dividing the Trp fluorescence intensity of the peptide/LUV solution alone (F_0) by the fluorescence intensity of the peptide/LUV solution in presence of different concentrations of quenching probes (F). Quenching constants K_{SV} were determined by linear regression using the Stern–Volmer equation for a dynamic process:

$$\frac{F_0}{F} = 1 + K_{SV}[Q] \quad (4)$$

where F and F_0 are the fluorescence intensities in presence and absence of acrylamide, respectively, and $[Q]$ is the total molar concentration of the quencher in the sample.

To gain information on the accessibility of the tryptophans in the lipid bilayer, we employed three different membrane-anchored quenching probes: NBD-PE as a probe for the bilayer surface [37], 5-doxyl stearic acid for the deeper interface region [38], and Br-PC for the lipophilic core of the bilayer [37,39]. Again, peptide solutions for a final concentration of 10 μM were added to vesicles composed of 1 mM phospholipid mixture of various POPG/POPC contents. The respective quenching probe was added from a 2-mM ethanolic stock solution, resulting in concentrations between 48 and 200 μM. After allowing the system to equilibrate, the intrinsic Trp fluorescence of the peptide was measured. The quenching constants K_{SV} were again determined by linear regression using the Stern–Volmer equation according to Eq. (4). Information about the localization of the peptides in phospholipid bilayers was derived by comparison of the F_0/F values for all four quenching probes.

2.7.2. Fluorescence polarization

To monitor the membrane perturbation upon addition of the peptides, we labeled the vesicles with the membrane-bound probes DPH or TMA-DPH, respectively. Both probes are nonfluorescent in aqueous media but partition readily into membranes and other lipid assemblies, accompanied by strong fluorescence enhancement. DPH is located in the membrane interior, whereas TMA-DPH is anchored to the surface by the trimethylammonium substituent. To prepare the samples, 2 μM DPH (from a 1 mM stock solution in acetonitrile) was added to LUVs composed of 1 mM phospholipid mixtures of various POPG/POPC contents. The samples were allowed to stand for 10 min before measurement. Increasing concentrations of peptides, from a 1 mM stock solution, were added to the samples. A polarization attachment (Varian, Mulgrave, Australia) was adapted to the Varian Cary Eclipse spectrofluorometer. Steady-state polarization P was determined according to the following equation [40]:

$$P = \frac{I_{VV} - GI_{VH}}{I_{VV} + GI_{VH}} \quad (5)$$

where I_{VV} is the emission intensity of vertically polarized light parallel to the plane of excitation and I_{VH} is the emission intensity of horizontally polarized light perpendicular to the plane of excitation. The instrumental factor G ($G = I_{HV}/I_{HH}$) was determined by measuring the polarized components of the probe's fluorescence with horizontally polarized excitation.

3. Results

3.1. Peptide design

An overview over all investigated peptides is given in Table 1. A systematic investigation of the internalisation efficiency of N-terminally truncated hCT derivatives in a MDCK cell model [19] revealed that hCT(18–32) is the shortest sequence that was internalised while hCT(9–32) turned out to be the most efficient derivative. In a ^{1}H NMR study, we found that hCT(9–32) contains two short α-helices interrupted by the central Pro (M. Herbig, unpublished data); A23-hCT(9–32) was synthesized to investigate the influence of a continuous α-helix on the properties of the peptide. W10-hCT(9–32) and W30-hCT(9–32) were synthesized with the intention to enhance membrane affinity of the peptides by means of replacing terminal Gly-residues by Trp showing enhanced affinity to phospholipid bilayers. Furthermore, the insertion of Trp allowed us to perform Trp quenching studies. This was also the intention for synthesizing W2-pVEC; we replaced a lipophilic Leu close to the N-terminus in order to change the peptide's physicochemical properties as little as possible.

3.2. Liposome–buffer partitioning experiments.

To test the propensity of hCT to interact with cell membranes, partition coefficients were determined in a liposome–buffer equilibrium system [33]. In contrast to partitioning studies in isotropic media, e.g., water/octanol, the choice of anisotropic media like liposomes also includes ionic interactions and, therefore, represents a more realistic model. The concept of anisotropic lipophilicity can be regarded as being an intermediate case between partitioning and binding [41]. LUVs were prepared by extrusion and their size distribution determined by dynamic light scattering (intensity distribution). All liposomes showed monomodal distributions, and their mean diameters were 103.4±1.9 nm for POPC LUVs and 83.8±0.3 nm for POPC/POPG (80:20) LUVs. A high excess of lipids (lipid/peptide molar ratio of 200) was chosen to avoid significant influence of membrane-bound peptides on the typical bilayer structure.

For the hCT derivatives, a pH of 3.5 was chosen to avoid potential aggregation of some of the peptides during the duration of the experiments. Apparent partition coefficients D were determined after 7 h. Fig. 1A demonstrates the resulting partition coefficients of various hCT-derived CPPs in neutral POPC LUVs. Owing to its hydrophobic C-terminal

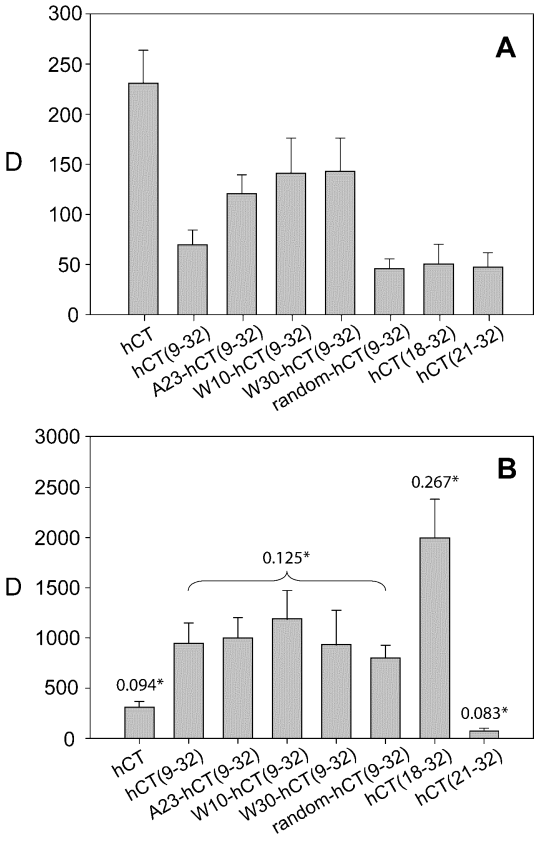

Fig. 1. Non-logarithmic representation of apparent liposome–buffer partition coefficients (D) between extruded LUVs and acidic acid/acetate buffer pH=3.5 at a total lipid concentration of 4 mM and a peptide concentration of 20 μM. (A) Pure POPC liposomes and (B) liposomes composed of POPC/POPG 80:20. The numbers labelled with an asterisk in (B) indicate the net positive charge per amino acid at pH 3.5.

part, the untruncated hCT showed a D value of about 220, which was higher than the D values of the truncated derivatives. The partition coefficient of hCT(9–32) increased by a factor of 2 when replacing the Gly in position 10 or 30 by a Trp. Trp is known to have the strongest membrane anchoring properties of all amino acids [42]. We were able to demonstrate by NMR experiments in DPC micelles at pH 5.5 that the replacement of the Pro in position 23 by an Ala led to the formation of a continuous α-helix (M. Herbig, unpublished data) and a 1.7-fold increase in D. The hCT(9–32) derivative with randomised amino acid composition (hCT-random) and more truncated derivatives had moderately reduced D values as compared to hCT(9–32).

Partition coefficients D of up to 2006 (log$D$ 3.30) were found in experiments with negatively charged POPC/POPG (80:20) LUVs (Fig. 1B). Unlike the experiments with neutral POPC, the extent of interaction was mainly governed by the density of positive charges in the peptide sequences. For hCT(18–32) with an average positive net charge per amino acid (c/AA) of 0.267, a D of 2006 was obtained, whereas hCT(21–32) with a c/AA ratio of 0.083 had a D of only 70. For hCT(9–32) and all of its modifications, irrespective of their sequence, D values in the range between 799 (random hCT(9–32)) and 1193 (W10-hCT(9–32)) were obtained. Whereas the D value of hCT remained almost unchanged, D values of hCT(9–32) and its modifications were increased up to 8- to 10-fold upon addition of 20% POPG; an even 40-fold increase was found with hCT(18–32). The obvious reason for the enhanced interaction of positively charged peptides is its electrostatic binding to the negatively charged lipid.

Partitioning experiments with pVEC and W2-pVEC were performed at a pH of 7.4 (Fig. 2). As compared to the hCT derivatives, D values were clearly higher in POPC LUVs, but only moderately higher with POPC/POPG (80:20). Typically, the enhancement of interaction due to negatively charged lipids was less pronounced as compared to hCT derivatives.

3.3. Acrylamide quenching

To determine the exposure of the Trp containing CPPs in LUV dispersions to the aqueous phase, we used the neutral hydrophilic quencher acrylamide to quench intrinsic Trp fluorescence. Acrylamide is unable to penetrate the hydrophobic membrane core and, therefore, non-polar fluorophores embedded in the bilayer cannot be quenched [43].

The studies were performed at pH 7.4 and 3.5 in LUVs composed of POPC, POPG, or a mixture (80:20) of both. As shown in Table 1, pAntp has two Trp residues (position 6 and 14), whereas W10-hCT(9–32), W30-hCT(9–32), and W2-pVEC have only one. The Trp fluorescence of all four CPPs followed the linear Stern–Volmer equation (Eq. (4)) for the quencher acrylamide. Table 2 shows the Stern–Volmer quenching constants $K_{SV}[M^{-1}]$ for W10-hCT(9–32), W30-hCT(9–32), W2-pVEC, and pAntp in POPC/POPG (80:20) and POPG LUVs in buffers of pH 7.4 and 3.5. In POPC/POPG high K_{SV} of 9 to 21 M^{-1} were found for the hCT derivatives, suggesting strong exposure to the water phase and, therefore, a more superficial localization. In both types

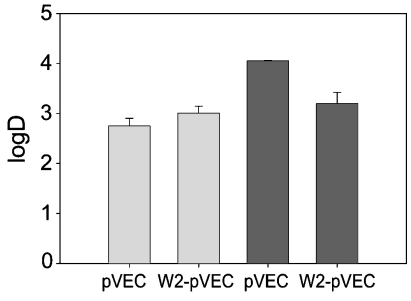

Fig. 2. Apparent liposome–buffer partition coefficients (log$D$) between extruded LUVs and PBS pH=7.4 at a total lipid concentration of 4 mM and a peptide concentration of 20 μM. Columns for pure POPC liposomes are represented in light grey and those for liposomes composed of POPC/POPG 80:20 in dark grey.

Table 2
Stern–Volmer constants K_{SV} for acrylamide quenching of tryptophan fluorescence

	Lipid	K_{SV} [M^{-1}]			
		W10-hCT (9–32)	W30-hCT (9–32)	W2-pVEC	pAntp
pH 7.4	POPC/POPG	9.38	15.17	2.94	1.81
	POPG	2.05	1.38	2.05	1.89
pH 3.5	POPG/POPG	15.69	20.63	0.72	3.13
	POPG	3.38	3.77	2.07	2.31

Increasing concentrations (10 mM to 100 mM) of acrylamide were added to LUVs incubated with different peptides, and K_{SV} were calculated according to Eq. (4). The lipid/peptide ratio was 100. Relative standard deviations were in the range of 1–5%.

of LUVs, quenching was somewhat more pronounced at pH 3.5 than pH 7.4, and quenching of W30-hCT(9–32) stronger than W10-hCT(9–32), suggesting a slightly weaker interaction. In POPG LUVs, K_{SV} values were largely decreased, indicating a much deeper insertion of the peptides. The cationic peptides W2-pVEC and pAntp showed low K_{SV} values, ranging from 0.7 to 3.1 M^{-1}, for all media, indicating that the peptides were buried to a large extent inside the bilayer. Fig. 3 depicts the percentage of the original fluorescence quenched after addition of 100 mM acrylamide; in this representation–

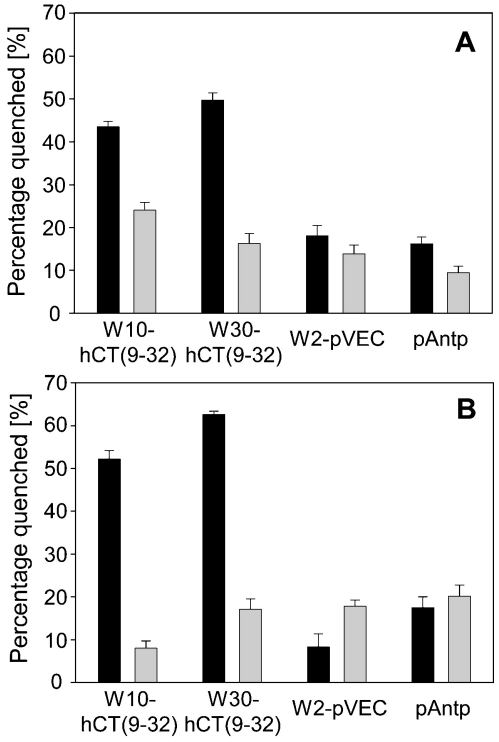

Fig. 3. Percentage of quenched intrinsic Trp fluorescence of various CPPs in LUVs at an acrylamide concentration of 100 mM. Filled columns represent LUVs composed of POPC/POPG (80:20) and grey columns LUVs of pure POPG. Experiments were performed in PBS buffer of pH 7.4 (A), or acetate buffer of pH 3.5 (B). Spectra were recorded at ambient temperature (approximately 22 °C). Results are represented as mean and standard deviation of three independent experiments.

especially for week and moderate quenching–differences in the effects became more apparent, which simplified the comparison of the extents of quenching. Interestingly, at pH 7.4, for both of these peptides, the quenching effects were slightly more pronounced in POPC/POPG (80:20) as compared to POPG, whereas the opposite was the case at pH 3.5.

3.4. Trp quenching with membrane-anchored quenchers

To obtain more precise information about the localization of the CPPs within the lipid bilayers, membrane-anchored probes were used to quench the intrinsic Trp fluorescence of the peptides inside the bilayer. In NBD-PE, the NBD group is covalently attached to the head group of a phosphatidylethanolamine molecule. Therefore, it acts as a probe for the polar head groups on the level of the phosphate groups in lipid bilayers [37,44,45]. 5-doxyl stearic acid is a probe for the deeper interface region [38], and 11,12-Br-PC for the lipophilic core of the bilayer [37,39]. The radius of quenching for brominated probes is 8–9 Å [46], whereas spin-labelled probes quench over a range of 11–12 Å [47,48]. Therefore, it was necessary to employ several quenchers located at different positions in the bilayer in order to convincingly predict the localization of the peptides. A summary of all K_{SV} values is given in Table 3.

In POPC/POPG (80:20) LUVs at pH 7.4 (Fig. 4A), NBD-PE–the quencher for the bilayer surface–led to a total

Table 3
Stern–Volmer constants K_{SV} for tryptophan fluorescence quenching of various membrane anchored quenching molecules

		K_{SV} [M^{-1}]			
		W10-hCT (9–32)	W30-hCT (9–32)	W2-pVEC	pAntp
POPG/POPC (80:20)					
pH 7.4	NBD-PE	26,467.0	33,107.5	69,413.6	41,793.9
	5-DSA	2874.9	3646.7	31,672.4	7723.6
	Br-PC	4359.8	7943.5	14,113.7	17,528.5
pH 3.5	NBD-PE	64,761.0	83,727.2	47,165.9	19,119.9
	5-DSA	1406.5	2166.7	516.3	903.3
	Br-PC	613.9	3802.9	505.9	1203.3
POPG					
pH 7.4	NBD-PE	4398.2	2889.3	295,473.0	181,815.0
	5-DSA	1341.4	679.3	18,193.3	7838.1
	Br-PC	432,627.0	19,710.0	5267.2	2093.1
pH 3.5	NBD-PE	14,420.6	17,704.3	7841.6	11,422.7
	5-DSA	13,553.6	7373.5	11,518.4	9493.7
	Br-PC	30,361.7	19,556.0	3100.3	1313.4

Increasing concentrations (50 μM to 200 μM) of quenchers were added to LUVs incubated with different CPPs, and K_{SV} were calculated according to Eq. (4)[a]. The lipid/peptide ratio was 100. Relative standard deviations were in the range of 1–6%.

[a] In cases of very efficient quenching (K_{SV} > 10 000), occasionally a plateau in the Stern–Volmer plot was obtained below the final quencher concentration of 200 μM. In that case, only the linear part of the curve was used to calculate the constants.

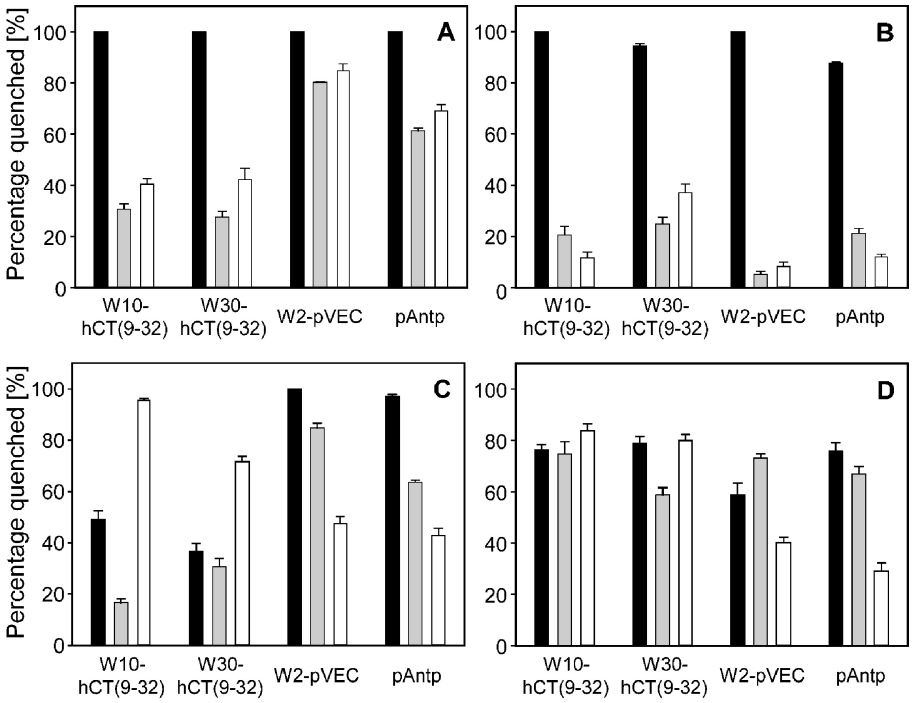

Fig. 4. Percentages of quenched intrinsic Trp fluorescence (100%: complete quenching; 0%: no effect) of various CPPs in LUVs. The quenching probes NBD-PE, 5-DSA, and Br-PC are represented in filled, grey, or open columns, respectively. The concentration of all quenchers was 100 μM, corresponding to a lipid/quencher ratio of 10. (A) LUVs composed of POPC/POPG (80:20) in PBS buffer of pH 7.4, (B) LUVs composed of POPC/POPG (80:20) in acetate buffer of pH 3.5, (C) LUVs composed of pure POPG in PBS buffer of pH 7.4, (D) LUVs composed of pure POPG in acetate buffer of pH 3.5. Spectra were recorded at ambient temperature (approximately 22 °C). Results are represented as mean and standard deviation of three independent experiments.

extinction of the fluorescence signal for all four peptides, whereas the more deeply inserted quenchers 5-DSA and Br-PC exhibited only moderate effects for W10-hCT(9–32), and W30-hCT(9–32), but strong effects for W2-pVEC and pAntp. This observation, in very good agreement with the acrylamide quenching data, led to the conclusion that the hCT-derived peptides were localized at the surface of the bilayer, while the cationic peptides remained in the upper region of the acyl chains of the phospholipids. At pH 3.5, the positive net charge–especially for hCT-derived CPPs–was elevated. As a consequence, NBD-PE effects at pH 3.5 were partially reduced but remained high (Fig. 4B), while 5-DSA and Br-PC effects were clearly decreased, indicating a shallower localization of all investigated CPPs.

In highly negatively charged POPG LUVs (Fig. 4C and D), the Br-PC effects were high for the hCT derivatives at pH 7.4, whereas effects of NDB-PE, but also of the interface probe 5-DSA, were comparably low. These findings, along with poor acrylamide quenching, led to the conclusion that these two peptides were more intensely buried in the hydrophobic region of the membrane, albeit not in the core of the bilayer. In this case, differences to pH 3.5 were less pronounced than in the POPC/POPG (80:20) system. Again, Br-PC showed very efficient quenching, but also NBD-PE and 5-DSA quenched between 60% and 80% of Trp fluorescence, suggesting insertion close to the 5-DSA spin label position in the upper region of the acyl chains. Also, W2-pVEC and pAntp show no pronounced differences between pH 7.4 and 3.5. Thus, both peptides resided in the upper acyl chain region. Data of the membrane-anchored quenchers allow no clear decision, at which pH the peptides reside closer to the interface region, but the acrylamide results suggested that at a pH of 3.5, there was a somewhat higher exposure to the water phase and, therefore, the localization of the peptides was more closely to the interface.

In neutral LUVs composed of pure POPC, hCT derivatives were only moderately quenched by NPD-PE, while 5-DSA and Br-PC exhibited week effects only (Fig. 5). W2-pVEC and pAntp showed higher NBD-PE effects, whereas the deeper quenchers also caused only minimal effects (data not shown).

In general, this study demonstrates that both, the two hCT-derived peptides on the one hand, and the two oligocationic peptides on the other, showed surprisingly similar behaviour. W10-hCT(9–32) and W30-hCT(9–32) demonstrated a conspicuous difference between POPG/POPC (80:2) LUVs, where they were located close to the bilayer surface, and those with POPG, with a deeper insertion towards the range of the hydrophobic acyl chains. Furthermore, there was an expected trend towards a slightly more superficial localization at pH 3.5 as compared to pH 7.4.

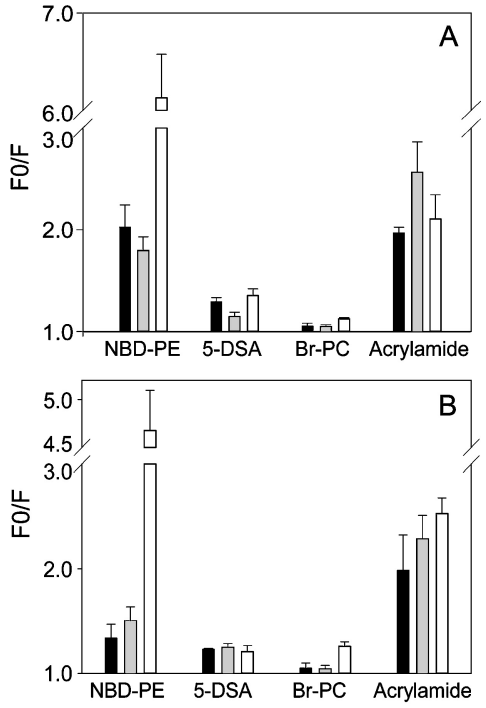

Fig. 5. Comparison of quenching effects in different uncharged membrane mimicking media. POPC LUVs are represented in filled columns, POPC SUVs in grey, and DPC micelles in open columns. The extent of Trp fluorescence quenching is shown by dividing the fluorescence without quencher (F_0) through the fluorescence after addition of 200 μM of membrane anchored quenchers, or 100 mM acrylamide, respectively. (A) Effects of W10-hCT(9–32), and (B) effects of W30-hCT(9–32), both in PBS buffer, pH 7.4. Spectra were recorded at ambient temperature (approximately 22 °C). Results are represented as mean and standard deviation of three independent experiments.

3.5. Comparison of quenching effects in LUVs, SUVs, and micelles

In literature, there is a large variety of different membrane-mimicking models to study peptide–bilayer membrane interactions, using LUVs [17,49–51], SUVs [29–31], and micelles [26,52–55]. However, as these models feature different physical–chemical properties, their results may depend on the chosen model. In particular, SUVs and especially DPC micelles are characterized by lower surface pressures due to their higher surface curvature. With respect to W10-hCT(9–32) and W30-hCT(9–32), we compared quenching effects of acrylamide and the membrane-anchored quenchers NBD-PE, 5-DSA, and Br-PC in POPC LUVs, POPC SUVs, and DPC micelles. We found no clear differences between LUVs and SUVs. In DPC micelles, effects of the surface-bound quencher NBD-PE were strongly increased, whereas only slight differences were determined for Br-PC, and no differences for acrylamide and 5-DSA. Expectedly, these findings indicate that peptide solutes integrated more likely into the less tightly packed surface of DPC micelles than into the bilayers of liposomes.

3.6. Fluorescence polarization

The polarization of the membrane-bound fluorophores DPH was used to estimate the internal microviscosity of bilayer membranes. By this means, effects of CPPs on membrane order and fluidity can be detected. DPH is non-fluorescent in aqueous dispersion but partitions readily into lipid membranes with lipid–water partition coefficients K_p of 1.3×10^6, accompanied by strong fluorescence enhancement [56]. Previously, the localization of DPH was found to be close to the centre of a lipid bilayer [57,58]. The polarization of the DPH probe was measured after the addition of increasing concentrations of CPP solutions in LUVs with varying negative charge density in PBS buffer at pH 7.4.

Fig. 6 shows DPH fluorescence polarization dependent on peptide concentration in POPG LUVs. The highly cationic CPPs pVEC, W2pVEC, and pAntp showed an increase in fluorescence polarization P from 0.13 for blank liposomes to approximately 0.19 at a concentration of 0.1 mM, i.e., a peptide/lipid ratio of 0.1. For all hCT-derived peptides, no significant effects could be found. In POPC as well as in POPC/POPG (80:20) liposomes, none of the investigated peptides caused significant effects. These findings led us to the conclusion that strong electrostatic interactions are required to cause a distinctive increase in DPH polarization.

3.7. ζ-potential measurements

The ζ-potential describes the electric potential of particles in aqueous solution at the shear plane close to their surface. Neutral LUVs have a ζ-potential slightly below zero and POPC/POPG LUVs at about −50 mV in very diluted buffers. If charged solutes bind to the surface of liposomes, a shift in ζ-potential can be expected. Because buffers of high ionic strength lead to a reduction of the ζ-potential, a very dilute phosphate buffer (1 mM, pH 7.4) was used. Fig. 7 shows an

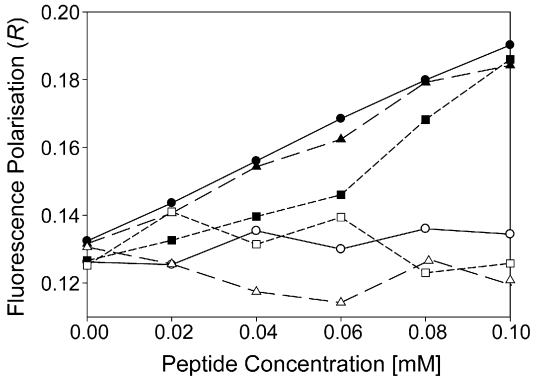

Fig. 6. Fluorescence polarization of DPH labelled POPG LUVs as a function of concentrations of different CPPs. The peptides pVEC (▲), W2-pVEC (●), pAntp (■), hCT(9–32) (□), W10-hCT(9–32) (○), and W30-hCT(9–32) (Δ) were added to LUV dispersion in PBS (pH 7.4) containing 2 mM DPH. Spectra were recorded at ambient temperature (approximately 22 °C).

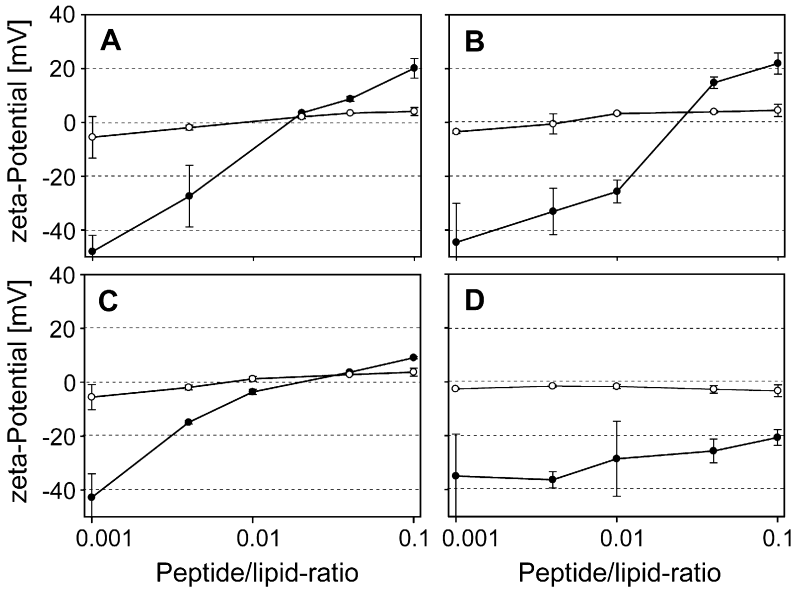

Fig. 7. Effects of different CPPs on the ζ-potential of POPC/POPG (80:20) LUVs (●) and POPC LUVs (○). Different concentrations of (A) pVEC, (B) W2-pVEC, (C) pAntp, and (D) hCT(9–32) were added to a 50-mM solution of LUV in a 1 mM PBS buffer, pH 7.4. Measurements were performed at ambient temperature (approximately 22 °C). Results are represented as mean and standard deviation of three independent experiments.

increase in ζ-potential with POPC and POPG/POPC (80:20) liposomes when adding increasing concentrations of various CPPs. As expected, pVEC (Fig. 7A) and W2-pVEC (Fig. 7B) caused very similar effects; in both cases the ζ-potential of POPC/POPG (80:20) LUVs was increased from about −45 mV to 20 mV at a peptide/lipid ratio of 0.1. For neutral POPC liposomes, only a slight rise from about −5 mV to 5 mV was observed. Also, pAntp (Fig. 7C) caused comparable effects, except for a flatter curve for POPC/POPG (80:20). As expected, hCT(9–32)with a net charge of +1 at pH 7.4, gave rise to a ζ-potential increase to −20 mV only in POPG/POPC (80:20) LUVs, whereas a slight but insignificant increase could be observed in POPG LUVs. Obviously, the small net charge of hCT(9–32) is incapable to compensate the large charge density of POPG LUVs. The modifications W10-hCT(9–32) and W30-hCT(9–32) showed no significant differences as compared to hCT(9–32) (data not shown).

4. Discussion

Over the past years, the field of CPP research experienced a shift of its major paradigm: the intriguing idea of an energy independent, passive pathway of CPPs through biomembranes, playing a predominant role in earlier CPP studies [9–11], has been increasingly abolished in favour of the involvement of endocytosis [3–6,12]. In several studies, a two-step process was suggested, involving initial adherence and enrichment at or in the phospholipid bilayer, which may subsequently trigger endocytosis [3,5,12–14].

Whereas sufficient proof for an uptake of hCT-derived peptides [19,20,34] as well as for pVEC [22,23] has been demonstrated in a variety of cellular models, as yet only limited information is accessible about their interaction with the lipid membrane, leaving the biophysical background to their cellular internalization largely elusive. Biophysical studies on the interaction of CPPs with biomembranes are expected to deepen the mechanistic understanding of the first step in CPP internalisation. Here, we focus on interactions with established bilayer models employing four independent methodologies, namely liposome–buffer partitioning, ζ-potential measurements, tryptophane fluorescence quenching, and fluorescence polarization.

We compared hCT(9–32) and a series of derivatives thereof, representing a class of weakly cationic peptides equipped with a hydrophobic C-terminal domain on the one hand, with two oligocationic CPPs, pVEC and pAntp (penetratin), on the other hand. In contrast to the endocytic uptake of hCT-derived peptides [19,20,34], Elmqvist et al. proposed a non-endocytic, passive mechanism for pVEC [5,22,23]. The authors draw their hypothesis from (i) reduced uptake at 4 °C, in combination with (ii) positive uptake of an all-D analogue of pVEC. Numerous uptake studies have been performed to elucidate the cellular uptake of pAntp. Early publications proposed passive uptake via inverted micelles [2,24] (and references therein), but more recent ones suggest endocytic uptake [15,16,59]. Even consecutive contributions of the two mechanisms have been proposed [27,60]. Passive pAntp permeation through lipid bilayers was demonstrated for giant unilamellar vesicles (GUVs) only [10,31], but not for LUVs [10,31]. GUVs show undulated membrane structures differing considerably from LUVs [31,61].

Our liposome–buffer partition experiments demonstrated marked to high affinities of hCT-derived peptides to both

negatively charged and even neutral bilayers. Expectedly, the affinities to POPC LUVs decreased with increasing molecular size of the derivatives, and increased when Gly was replaced by the more lipophilic Trp. The lower partition coefficient of the random sequence as compared to the hCT-derived peptides demonstrated that, additional to amino acid sequence, secondary structure may play an equally significant role for their affinity to phospholipid membranes. In contrast, the interaction of the hCT-derived CPPs with negatively charged POPC/POPG LUVs was governed by the ratio of positive charges per amino acid. Generally, the affinity to negatively charged lipid membranes was particularly enhanced. Remarkably, partition coefficients of pVEC in both POPC and POPC/POPG liposomes were about 10-fold higher than with hCT(9–32).

To our knowledge, liposome–buffer equilibrium dialysis was not yet considered for studying CPPs. In contrast to binding studies, utilizing the blue shift in Trp fluorescence emission [49,62] caused by the interaction of Trp with a hydrophobic environment, liposome–buffer equilibrium dialysis offers a more general tool to monitor various types of peptide–bilayer interactions, even mere association on or with the outer bilayer surface. Nevertheless, because of its unspecific nature, the data need to be interpreted in concert with more specific assays. Our assumption of a superficial localization of hCT-derived CPPs on neutral bilayers is supported by the low Trp fluorescence quenching in pure POPC (Fig. 5), in combination with moderate effects of the interface quenchers and strong quenching of acrylamide. Concomitantly, effects on the deep quencher were negligible.

A schematic summary of the Trp quenching studies in terms of the CPPs' localization in bilayers is given in Fig. 8. Interestingly, not only the two hCT-derived peptides on the one hand, but also the two oligocationic peptides, pVEC and pAntp, on the other hand, show similar localization in the respective buffers and phospholipid compositions. W10-hCT(9–32) and W30-hCT(9–32) stay at the interface of POPC/POPG (80:20) bilayers with partial exposure to the surrounding aqueous phase, but penetrate more deeply into the hydrophobic region of pure POPG bilayers. The deep penetration into highly negatively charged bilayers may be explained by the low positive net charge and relative hydrophobicity of hCT-derived peptides causing anchorage in the hydrophobic core of the membrane, whereas the high redundancy in positively charged amino acids of the two oligocationic CPPs is likely to restrict insertion into the deeper interface/upper acyl chain region. However, at no instance were the peptides found to be localized in the innermost core of the bilayer.

Electrostatic attraction to negatively charged phospholipids prior to insertion into the lipid membrane seems to be a prerequisite for all investigated CPPs, irrespective of charge density. This may be concluded from the generally somewhat shallower localization at pH 3.5 as compared to 7.4. Nevertheless, the pH effect is most pronounced with the oligocationic pVEC and pAntp in POPC/POPG and explained by an increased positive net charge at the lower pH. Our findings with pAnpt are in agreement with corresponding data in literature [17,30,31]: Likewise to the findings of Magzoub et al. [30], we found a slight reduction in the quenching constants of the deeper quenchers at high charge densities (pure POPG) as compared to lower charge densities (20% POPG in our study, 30% in the cited work). As compared to Christiaens et al. [17], however, we found distinctly higher quenching effects with the core quencher 11,12-Br-PC, which may be explained by the use of POPC/POPG (80:20) LUVs instead of PC/PS (70:30) SUVs in the work of Christiaens et al.

The LUV model system was chosen because of its superior resemblance to biological membranes. Cell membranes are characterized by a lipid packing density of 35 mN/m or slightly higher [63]. Whereas LUVs of 100 nm have lipid packing density of about 32 mN/m [64,65], SUVs of 30 nm have only about 23 mN/m [64], obviously because of their higher bilayer curvature. At reduced

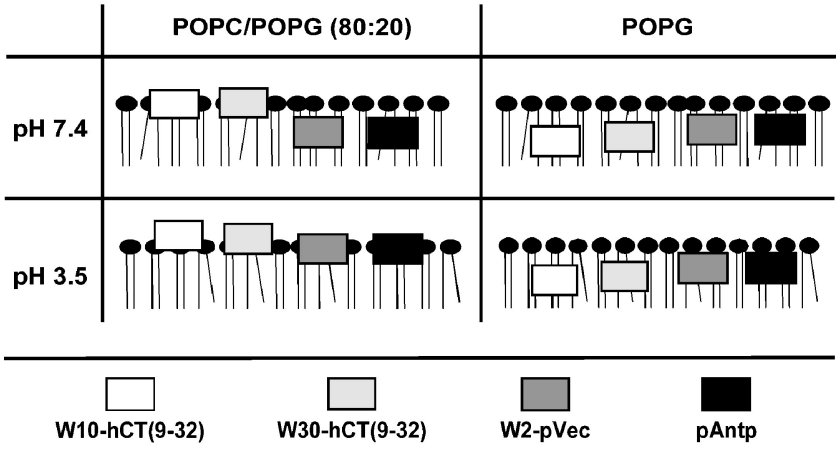

Fig. 8. Schematic representation for insertion of CPPs in POPC/POPG (80:20) and POPG LUVs at pH 7.4 or 3.5, respectively. The respective positions were estimated based on Trp fluorescence quenching data from Tables 2 and 3 and Figs. 3 and 4.

surface pressure, insertion of solutes is more likely. In fact, anomalous peptide binding to SUVs has been reported in literature [66]. Despite, we found no significant differences between SUVs and LUVs concerning the membrane-anchored quenchers, except for slightly higher acrylamide quenching observed with SUVs. Accordingly, we observed dramatically increased NBD-PE quenching and a significantly higher Br-PC quenching rate when using lipid micelles, which are characterized by lipid packing densities of about 10 mN/m [67], instead of LUVs. Although easier to prepare and in spite of their excellent physical stability, head group structure and packing of lipid micelles deviate markedly from those of biological membranes. The minor differences in the interaction of hCT-derived CPPs with the deep quenchers are the result of their superficial localization and cannot be extrapolated to deeply inserted CPP.

In the DPH polarization studies, again a profound difference between the weakly cationic hCT-derived peptides and the two oligocationic peptides pVEC and pAntp was observed. Whereas distinct polarization effects of the oligocationic CPPs were demonstrated in POPG LUVs, no significant effect for any of the hCT-derived peptides could be observed. Interestingly, in POPC/POPG (80:20), where the Trp fluorescence studies showed insertion towards the hydrophobic core, no change in polarization could be detected. Obviously, deep insertion alone is not sufficient to cause changes in the microviscosity of the bilayer and hence polarization. Our observation that polarization effects cannot be predicted by the depths of insertion is also supported by the work of Magzoub et al. who also found similar effects for pAntp [30]. Similarly, none of the investigated peptides showed any effects in POPC LUVs. So far, polarization effects in neutral liposomes could only be shown for transportan, owing to the fact that its C-terminal domain consists of the pore-forming wasp venom peptide mastoparan [30]. Several pore forming peptides like bak, the C-terminal sequence of the pro-apoptotic protein [68], and melittin (M. Herbig, unpublished data) have been found to disturb neutral lipid membranes and increase DPH polarization. Usually, pore-forming peptide agents elicit marked cellular toxicity [69,70]. Analysis of the ζ-potential provides further evidence for preferential interaction with (partially) negatively charged lipids as compared to neutral bilayers. Though, even with neutral lipids, the cationic peptides show a moderate, but significant interaction. Previous studies observed significant interactions of pAntp [17,30] and Tat-derived CPP [53] only with negatively charged vesicles. Our findings confirm that deeper penetration of pAntp (and possibly oligocationic CPPs in general) occurs only when the bilayers contains negatively charged lipids. Nevertheless, in addition to that, we also observed interactions with neutral POPC LUVs. Obviously, these interactions are of weaker nature and restricted to the outermost surface of the bilayer so that several methods commonly used in CPP research failed to detect them. This superficial association on the bilayer surface may be in line with the observation of Wagner et al. [71] who found no relevant insertion of hCT(9–32) into monolayers composed of neutral phospholipids.

Nevertheless, by combination of liposome–buffer equilibrium dialysis, ζ-potential measurements and Trp fluorescence quenching with the surface-anchored probe NBD-PE, demonstration of these interactions was successful. The fact that positively charged CPPs show an affinity even towards neutral phosphatidyl choline is not surprising because binding of positively charged solutes may lead to repellence of the positively charged end group of the choline towards the water phase [72]. This has been hypothesized by van Balen et al. to open the polar surface and allow the charged solute to interact with the interface region [41]. This would explain our findings.

All the investigated peptides' affinities were significantly higher when negatively charged lipids were present in the bilayer as compared to neutral lipids. Unlike the oligocationic CPPs, the hCT-derived peptides remained on the bilayer surface even in the presence of 20% POPG. However, as supported by strong evidence for endocytic uptake of hCT(9–32) in various cell models with predominantly neutral lipids [19,20], interfacial localization may be sufficient to trigger endocytosis.

Recently, Lundberg et al. concluded that the main feature of CPPs is to mediate the cell surface adherence. This was thought to occur after a first step of electrostatic interaction and is then followed by an uptake into endosomes [5]. Also, a correlation of cell surface association or membrane affinity and uptake efficiency could be observed [16] (M. Herbig et al., unpublished data). The manner and intensity of interaction, especially the pronounced interfacial localization, of all studied CPPs with lipid bilayers are better compatible with the idea of an endocytic uptake rather than the assumption of passive transport. This includes also pVEC, having pronounced similarities to pAntp. Elmquist et al. [22,23] proposed a non-endocytic uptake of pVEC, just based on uptake at 4 °C after fixation and the successful uptake of an all-D analogue of pVEC. Nevertheless, on this evidence alone, an endocytic contribution at 37 °C cannot be excluded. Even more so, in a subsequent study, Richard et al. [4] demonstrated that cell fixation, even under mild conditions, may lead to artifactual uptake of CPP. In fact, in a recent study, more specific investigations of the uptake of pVEC, namely ATP depletion experiments and intracellular localization studies, brought up strong evidence for endocytic uptake [73].

Pore formation as a possible mechanism of passive translocation could be excluded for pAntp [74] as well as for hCT derivatives and pVEC (M. Herbig, unpublished data). The higher affinity towards the interface as compared to the hydrophobic core and the strong enrichment in the interface of phospholipid bilayers made passive uptake unlikely. On the other hand, enrichment of CPPs at the interface, possibly

followed by aggregation, may have triggered endocytic uptake. Especially for hCT-derived CPPs, there is now strong evidence for endocytic uptake since several in vitro uptake studies [19,20,34] suggest this uptake mechanism. The previously published monolayer study [71] and the present bilayer study provide detailed insight into their interactions with the lipid membrane that are well consistent with this uptake mechanism.

Acknowledgements

This work was supported by the Commission of the European Union (EU project on Quality of Life and Management of Living Resources, Project No. QLK2-CT-2001-01451). The excellent support in mass spectrometry of R. Reppich, University of Leipzig, is kindly acknowledged. We thank Dr. Anna Seelig, Biozentrum Basel for carefully reviewing the manuscript.

References

[1] M. Lindgren, M. Hallbrink, A. Prochiantz, U. Langel, Cell-penetrating peptides, Trends Pharmacol. Sci. 21 (2000) 99–103.
[2] D. Derossi, G. Chassaing, A. Prochiantz, Trojan peptides: the penetratin system for intracellular delivery, Trends Cell. Biol. 8 (1998) 84–87.
[3] R. Trehin, H.P. Merkle, Chances and pitfalls of cell penetrating peptides for cellular drug delivery, Eur. J. Pharm. Biopharm. 58 (2004) 209–223.
[4] J.P. Richard, K. Melikov, E. Vives, C. Ramos, B. Verbeure, M.J. Gait, L.V. Chernomordik, B. Lebleu, Cell-penetrating peptides. A reevaluation of the mechanism of cellular uptake, J. Biol. Chem. 278 (2003) 585–590.
[5] M. Lundberg, S. Wikstrom, M. Johansson, Cell surface adherence and endocytosis of protein transduction domains, Mol. Ther. 8 (2003) 143–150.
[6] E. Vives, J.P. Richard, C. Rispal, B. Lebleu, TAT peptide internalization: seeking the mechanism of entry, Curr. Protein Pept. Sci. 4 (2003) 125–132.
[7] C. Foerg, U. Ziegler, J. Fernandez-Carneado, E. Giralt, R. Rennert, A.G. Beck-Sickinger, H.P. Merkle, Decoding the entry of two novel cell-penetrating peptides in HeLa cells: lipid raft-mediated endocytosis and endosomal escape, Biochemistry 44 (2005) 72–81.
[8] E.L. Snyder, S.F. Dowdy, Cell penetrating peptides in drug delivery, Pharm. Res. 21 (2004) 389–393.
[9] S.R. Schwarze, K.A. Hruska, S.F. Dowdy, Protein transduction: unrestricted delivery into all cells? Trends Cell Biol. 10 (2000) 290–295.
[10] P.E. Thoren, D. Persson, M. Karlsson, B. Norden, The antennapedia peptide penetratin translocates across lipid bilayers—The first direct observation, FEBS Lett. 482 (2000) 265–268.
[11] A. Prochiantz, Getting hydrophilic compounds into cells: lessons from homeopeptides, Curr. Opin. Neurobiol. 6 (1996) 629–634.
[12] J.S. Wadia, R.V. Stan, S.F. Dowdy, Transducible TAT-HA fusogenic peptide enhances escape of TAT-fusion proteins after lipid raft macropinocytosis, Nat. Med. 10 (2004) 310–315.
[13] A. Scheller, J. Oehlke, B. Wiesner, M. Dathe, E. Krause, M. Beyermann, M. Melzig, M. Bienert, Structural requirements for cellular uptake of alpha-helical amphipathic peptides, J. Pept. Sci. 5 (1999) 185–194.
[14] J. Oehlke, A. Scheller, B. Wiesner, E. Krause, M. Beyermann, E. Klauschenz, M. Melzig, M. Bienert, Cellular uptake of an alpha-helical amphipathic model peptide with the potential to deliver polar compounds into the cell interior non-endocytically, Biochim. Biophys. Acta 1414 (1998) 127–139.
[15] G. Drin, S. Cottin, E. Blanc, A.R. Rees, J. Temsamani, Studies on the internalisation mechanism of cationic cell-penetrating peptides, J. Biol. Chem. 278 (2003) 31192–31201.
[16] G. Drin, M. Mazel, P. Clair, D. Mathieu, M. Kaczorek, J. Temsamani, Physico-chemical requirements for cellular uptake of pAntp peptide. Role of lipid-binding affinity, Eur. J. Biochem. 268 (2001) 1304–1314.
[17] B. Christiaens, J. Grooten, M. Reusens, A. Joliot, M. Goethals, J. Vandekerckhove, A. Prochiantz, M. Rosseneu, Membrane interaction and cellular internalization of penetratin peptides, Eur. J. Biochem. 271 (2004) 1187–1197.
[18] S.L. Silverman, Calcitonin, Endocrinol. Metab. Clin. North. Am. 32 (2003) 273–284.
[19] R. Trehin, U. Krauss, R. Muff, M. Meinecke, A.G. Beck-Sickinger, H.P. Merkle, Cellular internalization of human calcitonin derived peptides in MDCK monolayers: a comparative study with Tat(47–57) and penetratin(43–58), Pharm. Res. 21 (2004) 33–42.
[20] R. Trehin, U. Krauss, A.G. Beck-Sickinger, H.P. Merkle, H.M. Nielsen, Cellular uptake but low permeation of human calcitonin-derived cell penetrating peptides and Tat(47–57) through well-differentiated epithelial models, Pharm. Res. 21 (2004) 1248–1256.
[21] R. Trehin, H.M. Nielsen, H.G. Jahnke, U. Krauss, A.G. Beck-Sickinger, H.P. Merkle, Metabolic cleavage of cell penetrating peptides in contact with epithelial models: human calcitonin (hCT) derived peptides, Tat(47–57) and Penetratin(43–58), Biochem. J. 382 (2004) 945–956.
[22] A. Elmquist, U. Langel, In vitro uptake and stability study of pVEC and its all-D analog, Biol. Chem. 384 (2003) 387–393.
[23] A. Elmquist, M. Lindgren, T. Bartfai, U. Langel, VE-cadherin-derived cell-penetrating peptide, pVEC, with carrier functions, Exp. Cell Res. 269 (2001) 237–244.
[24] A. Prochiantz, Homeodomain-derived peptides. In and out of the cells, Ann. N.Y. Acad. Sci. 886 (1999) 172–179.
[25] D. Derossi, S. Calvet, A. Trembleau, A. Brunissen, G. Chassaing, A. Prochiantz, Cell internalization of the third helix of the Antennapedia homeodomain is receptor-independent, J. Biol. Chem. 271 (1996) 18188–18193.
[26] K. Kilk, M. Magzoub, M. Pooga, L.E. Eriksson, U. Langel, A. Graslund, Cellular internalization of a cargo complex with a novel peptide derived from the third helix of the islet-1 homeodomain. Comparison with the penetratin peptide, Bioconjug. Chem. 12 (2001) 911–916.
[27] G. Dom, C. Shaw-Jackson, C. Matis, O. Bouffioux, J.J. Picard, A. Prochiantz, M.P. Mingeot-Leclercq, R. Brasseur, R. Rezsohazy, Cellular uptake of Antennapedia Penetratin peptides is a two-step process in which phase transfer precedes a tryptophan-dependent translocation, Nucleic Acids Res. 31 (2003) 556–561.
[28] S. Boichot, U. Krauss, T. Plenat, R. Rennert, P.E. Milhiet, A. Beck-Sickinger, C. Le Grimellec, Calcitonin-derived carrier peptide plays a major role in the membrane localization of a peptide–cargo complex, FEBS Lett. 569 (2004) 346–350.
[29] M. Magzoub, L.E. Eriksson, A. Graslund, Conformational states of the cell-penetrating peptide penetratin when interacting with phospholipid vesicles: effects of surface charge and peptide concentration, Biochim. Biophys. Acta 1563 (2002) 53–63.
[30] M. Magzoub, L.E. Eriksson, A. Graslund, Comparison of the interaction, positioning, structure induction and membrane perturbation of cell-penetrating peptides and non-translocating variants with phospholipid vesicles, Biophys. Chem. 103 (2003) 271–288.
[31] B. Christiaens, S. Symoens, S. Verheyden, Y. Engelborghs, A. Joliot, A. Prochiantz, J. Vandekerckhove, M. Rosseneu, B. Vanloo, S. Vanderheyden, Tryptophan fluorescence study of the interaction of

penetratin peptides with model membranes, Eur. J. Biochem. 269 (2002) 2918–2926.
[32] U. Krauss, F. Kratz, A.G. Beck-Sickinger, Novel daunorubicin-carrier peptide conjugates derived from human calcitonin segments, J. Mol. Recognit. 16 (2003) 280–287.
[33] G.M. Pauletti, H. Wunderli-Allenspach, Partition-coefficients in-vitro-artificial membranes as a standardized distribution model, Eur. J. Pharm. Sci. 1 (1994) 273–282.
[34] M.C. Schmidt, B. Rothen-Rutishauser, B. Rist, A. Beck-Sickinger, H. Wunderli-Allenspach, W. Rubas, W. Sadee, H.P. Merkle, Translocation of human calcitonin in respiratory nasal epithelium is associated with self-assembly in lipid membrane, Biochemistry 37 (1998) 16582–16590.
[35] C. Ottiger, H. Wunderli-Allenspach, Partition behaviour of acids and bases in a phosphatidylcholine liposome–buffer equilibrium dialysis system, Eur. J. Pharm. Sci. 5 (1997) 223–231.
[36] R.H. Buck, F. Maxl, A validated HPLC assay for salmon calcitonin analysis. Comparison of HPLC and biological assay, J. Pharm. Biomed. Anal. 8 (1990) 761–769.
[37] F.S. Abrams, E. London, Calibration of the parallax fluorescence quenching method for determination of membrane penetration depth: refinement and comparison of quenching by spin-labeled and brominated lipids, Biochemistry 31 (1992) 5312–5322.
[38] P. Damberg, J. Jarvet, A. Graslund, Micellar systems as solvents in peptide and protein structure determination, Methods Enzymol. 339 (2001) 271–285.
[39] T.J. McIntosh, P.W. Holloway, Determination of the depth of bromine atoms in bilayers formed from bromolipid probes, Biochemistry 26 (1987) 1783–1788.
[40] J.R. Lakowicz, Principles of Fluorescence Spectroscopy, 2nd ed., Kluwer Academic, New York, 1999, pp. 291–303.
[41] G.P. van Balen, C.M. Martinet, G. Caron, G. Bouchard, M. Reist, P.A. Carrupt, R. Fruttero, A. Gasco, B. Testa, Liposome/water lipophilicity: methods, information content, and pharmaceutical applications, Med. Res. Rev. 24 (2004) 299–324.
[42] S.H. White, W.C. Wimley, Hydrophobic interactions of peptides with membrane interfaces, Biochim. Biophys. Acta 1376 (1998) 339–352.
[43] F. Moro, F.M. Goni, M.A. Urbaneja, Fluorescence quenching at interfaces and the permeation of acrylamide and iodide across phospholipid bilayers, FEBS Lett. 330 (1993) 129–132.
[44] H. Raghuraman, S.K. Pradhan, A. Chattopadhyay, Effect of urea on the organization and dynamics of triton X-100 micelles: a fluorescence approach, J. Phys. Chem. B 108 (2004) 2489–2496.
[45] F.S. Abrams, E. London, Extension of the parallax analysis of membrane penetration depth to the polar region of model membranes: use of fluorescence quenching by a spin-label attached to the phospholipid polar headgroup, Biochemistry 32 (1993) 10826–10831.
[46] E.J. Bolen, P.W. Holloway, Quenching of tryptophan fluorescence by brominated phospholipid, Biochemistry 29 (1990) 9638–9643.
[47] A. Chattopadhyay, E. London, Parallax method for direct measurement of membrane penetration depth utilizing fluorescence quenching by spin-labeled phospholipids, Biochemistry 26 (1987) 39–45.
[48] E. London, G.W. Feigenson, Fluorescence quenching in model membranes: 1. Characterization of quenching caused by a spin-labeled phospholipid, Biochemistry 20 (1981) 1932–1938.
[49] D. Persson, P.E. Thoren, M. Herner, P. Lincoln, B. Norden, Application of a novel analysis to measure the binding of the membrane-translocating Peptide penetratin to negatively charged liposomes, Biochemistry 42 (2003) 421–429.
[50] D. Persson, P.E. Thoren, B. Norden, Penetratin-induced aggregation and subsequent dissociation of negatively charged phospholipid vesicles, FEBS Lett. 505 (2001) 307–312.
[51] A. Agirre, C. Flach, F.M. Goni, R. Mendelsohn, J.M. Valpuesta, F. Wu, J.L. Nieva, Interactions of the HIV-1 fusion peptide with large unilamellar vesicles and monolayers. A cryo-TEM and spectroscopic study, Biochim. Biophys. Acta 1467 (2000) 153–164.
[52] M. Lindberg, J. Jarvet, U. Langel, A. Graslund, Secondary structure and position of the cell-penetrating peptide transportan in SDS micelles as determined by NMR, Biochemistry 40 (2001) 3141–3149.
[53] A. Ziegler, X.L. Blatter, A. Seelig, J. Seelig, Protein transduction domains of HIV-1 and SIV TAT interact with charged lipid vesicles. Binding mechanism and thermodynamic analysis, Biochemistry 42 (2003) 9185–9194.
[54] M. Lindberg, H. Biverstahl, A. Graslund, L. Maler, Structure and positioning comparison of two variants of penetratin in two different membrane mimicking systems by NMR, Eur. J. Biochem. 270 (2003) 3055–3063.
[55] L. Chaloin, P. Vidal, A. Heitz, N. Van Mau, J. Mery, G. Divita, F. Heitz, Conformations of primary amphipathic carrier peptides in membrane mimicking environments, Biochemistry 36 (1997) 11179–11187.
[56] Z.J. Huang, R.P. Haugland, Partition coefficients of fluorescent probes with phospholipid membranes, Biochem. Biophys. Res. Commun. 181 (1991) 166–171.
[57] R.D. Kaiser, E. London, Location of diphenylhexatriene (DPH) and its derivatives within membranes: comparison of different fluorescence quenching analyses of membrane depth, Biochemistry 38 (1999) 2610.
[58] S. Wang, J.M. Beechem, E. Gratton, M. Glaser, Orientational distribution of 1,6-diphenyl-1,3,5-hexatriene in phospholipid vesicles as determined by global analysis of frequency domain fluorimetry data, Biochemistry 30 (1991) 5565–5572.
[59] S. Console, C. Marty, C. Garcia-Echeverria, R. Schwendener, K. Ballmer-Hofer, Antennapedia and HIV transactivator of transcription (TAT) "protein transduction domains" promote endocytosis of high molecular weight cargo upon binding to cell surface glycosaminoglycans, J. Biol. Chem. 278 (2003) 35109–35114.
[60] M. Hallbrink, A. Floren, A. Elmquist, M. Pooga, T. Bartfai, U. Langel, Cargo delivery kinetics of cell-penetrating peptides, Biochim. Biophys. Acta 1515 (2001) 101–109.
[61] A. Fischer, T. Oberholzer, P.L. Luisi, Giant vesicles as models to study the interactions between membranes and proteins, Biochim. Biophys. Acta 1467 (2000) 177–188.
[62] P.E. Thoren, D. Persson, E.K. Esbjorner, M. Goksor, P. Lincoln, B. Norden, Membrane binding and translocation of cell-penetrating peptides, Biochemistry 43 (2004) 3471–3489.
[63] H. Brockman, Lipid monolayers: why use half a membrane to characterize protein–membrane interactions? Curr. Opin. Struct. Biol. 9 (1999) 438–443.
[64] H. Schindler, Formation of planar bilayers from artificial or native membrane vesicles, FEBS Lett. 122 (1980) 77–79.
[65] A. Seelig, Local anesthetics and pressure: a comparison of dibucaine binding to lipid monolayers and bilayers, Biochim. Biophys. Acta 899 (1987) 196–204.
[66] A.S. Ladokhin, S. Jayasinghe, S.H. White, How to measure and analyze tryptophan fluorescence in membranes properly, and why bother? Anal. Biochem. 285 (2000) 235–245.
[67] A. Seelig, Interaction of a substance P agonist and of substance P antagonists with lipid membranes. A thermodynamic analysis, Biochemistry 31 (1992) 2897–2904.
[68] M. Martinez-Senac Mdel, S. Corbalan-Garcia, J.C. Gomez-Fernandez, The structure of the C-terminal domain of the pro-apoptotic protein Bak and its interaction with model membranes, Biophys. J. 82 (2002) 233–243.
[69] K. Matsuzaki, Magainins as paradigm for the mode of action of pore forming polypeptides, Biochim. Biophys. Acta 1376 (1998) 391–400.
[70] K. Matsuzaki, S. Yoneyama, K. Miyajima, Pore formation and translocation of melittin, Biophys. J. 73 (1997) 831–838.
[71] K. Wagner, N. Van Mau, S. Boichot, A.V. Kajava, U. Krauss, C. Le Grimellec, A. Beck-Sickinger, F. Heitz, Interactions of the human calcitonin fragment 9–32 with phospholipids: a monolayer study, Biophys. J. 87 (2004) 386–395.
[72] H.D. Bauerle, J. Seelig, Interaction of charged and uncharged calcium

channel antagonists with phospholipid membranes. Binding equilibrium, binding enthalpy, and membrane location, Biochemistry 30 (1991) 7203–7211.
[73] P. Saalik, A. Elmquist, M. Hansen, K. Padari, K. Saar, K. Viht, U. Langel, M. Pooga, Protein cargo delivery properties of cell-penetrating peptides. A comparative study, Bioconjug. Chem. 15 (2004) 1246–1253.
[74] G. Drin, H. Demene, J. Temsamani, R. Brasseur, Translocation of the pAntp peptide and its amphipathic analogue AP-2AL, Biochemistry 40 (2001) 1824–1834.